The Implementation of an Activated Temperature Dependent Wall Boiling Model in an Eulerian-Eulerian Computational Fluid Dynamic Approach for Predicting the Wall Boiling Process

Originally published:

August 2018

Nuclear Technology 205(2018), 23-32

DOI: https://doi.org/10.1080/00295450.2018.1496693

The Implementation of an Activated Temperature Dependent Wall Boiling Model in an Eulerian-Eulerian Computational Fluid Dynamic Approach for Predicting the Wall Boiling Process

Wei Ding [1,2], Eckhard Krepper [2], Uwe Hampel [1,2]

[1] Institute of Fluid Dynamics, Helmholtz-Zentrum Dresden-Rossendorf, Dresden, Germany
[2]AREVA Endowed Chair of Imaging Techniques in Energy and Process Engineering, Technische Universität Dresden, Germany
w.ding@hzdr.de

ABSTRACT

In this work, we report on a development of time averaged Eulerian multiphase approach applied in the wall boiling process especially in the forced convective boiling process. Recently in order to get accurate bubble dynamics and reduce the case dependency, a single bubble model for nucleate boiling based on the known published models was developed. The model considers geometry change and dynamic contact and inclination angles during the bubble growth. The model has a good agreement with experiments. However the predicted bubble dynamics is wall superheat (cavity activation temperature) dependent. This single bubble model requires an update of the current nucleation site activation and heat partitioning models in time averaged Eulerian multiphase approaches. In this work, we will introduce this implementation in detail. Further with help of the multiple size group (MUSIG) model and a breakup and coalescence model, the time averaged Eulerian approach could simulate the bubble size distribution in a heated pipe. With the necessary calibration of the nucleation site density the comparisons between the calculation results and the Bartolomej's experiments demonstrate the success of the implementation and the accuracy of this approach.

KEYWORDS

Wall boiling; Eulerian multi-phase approach; microlayer; cavity group activation; updated heat partitioning

I. INTRODUCTION

Boiling and two phase flow involves mass, momentum and energy transfer at the liquid-vapor interface and further involves heat conduction into solid walls. These complex phenomena bring much more difficulties to understand, model and predict the boiling process with Computational Fluid Dynamics (CFD). Currently the most widely used approach to model the boiling process is the Eulerian two fluid framework of interpenetrating continua [1, 2]. In this approach, the equations of mass, momentum and energy are taken for each phase separately and weighted by volume fraction which represents the local ensemble averaged probability of occurrence of each phase. However in such a model, all the information on and about the interface structure is lost due to the averaging process [3]. Consequently, models are required to describe the interphase exchanges of the mass, momentum and energy. These models appear as some terms of the balanced equations. For the case of wall boiling, a wall boiling model, which can describe the heat transfer from heated wall to the bulk liquid, is strongly required. The heat partitioning models, such as RPI (Rensselaer Polytechnic Institute) model developed by Kurul and Podowski [4] in 1990, have been widely adopted in CFD codes to date. The heat flux from the wall is there portioned into contributions of liquid convection, quenching and evaporation. The quenching and evaporation terms are calculated from several parameters, such as active nucleation site density, the bubble departure diameter and bubble departure frequency. In this approach the proper consideration of the bubble dynamics such as the bubble departure diameter and bubble departure frequency further the nucleation site density on the heated wall is particularly important. Currently these important variables are predicted normally through empirical correlations. For example, the bubble departure diameter is usually calculated from the correlations of Tolubinsky and Kostanchuk [5], which give the bubble departure diameter as a function of sub-cooling. Also for the bubble waiting time and bubble frequency, Tolubinsky and Kostanchuk consider the constant ratio of waiting time and total time, with the waiting time being 80% of the bubble detachment period. However the correlations were developed from pool boiling experiments under 1 atmospheric pressure. They are highly problem-specific and require careful consideration with respect to their scope of application. In 2013, a CFD approach coupling the wall heat partitioning model (RPI) and population models so called Multiple size group (MUSIG) and inhomogeneous Multiple size group (iMUSIG) was introduced by Krepper et al. [2, 6, 7] which tracks bubbles with coalescence and breakup and was recently extended to evaporation and condensation. In the paper, they assessed the necessary recalibration of the empirical correlations for the specific experimental data.

Nevertheless currently the applied Eulerian CFD approach is still far away from being a predictive tool due to the correlation based bubble dynamics. A critical review by Krepper et al. in 2013 [2] of the employed correlations shows that some of the parameters are not suited for a broad usage for different fluids or different pressure levels but have to be carefully recalibrated for the intended applications. In our previous study [8] a single bubble model was developed to simulate and predict the bubble departure or lift-off during pool or flow boiling which will be shortly introduced later. The model includes more physics than the empirical correlations. The sub-model is rather case independent, which means there is no need for recalibration under different conditions as mentioned above.

In this work, the well-developed single bubble model was implemented in the Eulerian CFD approach. The new activation mechanism and heat flux partitioning were employed in order to enhance the performance and improve the prediction accuracy. Further the CFD approaches are compared and validated against different experimental cases.

II. State of the Art of the Submodels

As mentioned above, submodels are required to complete the missing information in the Eulerian-Eulerian (EE) CFD approach. For wall boiling processes, as one of the most popular models, the RPI model is often employed as a submodel to describe the bubble dynamics on the wall, cavity activation law and the heat partitioning.

The bubble dynamics is commonly described by the bubble departure / lift-off diameter and bubble generation frequency. It is quantified by two correlations in the RPI model in ANSYS CFX. One correlation is derived from the investigations by Tolubinsky and Kostanchuk [5] for water at different pressures and subcooling. The correlation is given as

$$d_W = d_{ref} e^{-\frac{T_{sat} - T_L}{\Delta T_{refd}}} , \quad (1)$$

where d_w is the bubble departure diameter , T_{sat} is saturation temperature and T_L is subcooling temperature obtained by evaluating the non-dimensional temperature profile of Kader [9] at a fixed value of y^+. y^+ is a defined as a dimensionless wall distance for a wall bounded flow $y^+ \equiv \frac{u_* y}{\nu}$. u_* is the friction velocity at the nearest wall, y is the distance to the wall and ν is kinematic viscosity. d_{ref} and ΔT_{refd} are parameters, which require adjustment for different cases [7]. From the assessment of Krepper, usually ΔT_{refd} is set to 45 K while d_{ref} is cased dependent. For example, in Krepper and Rzehak (2011) [7] with reference to the DEBORA case, d_{ref} was set to d_{ref} = 0.24 mm and d_{ref} = 0.35 mm at pressures of 2.62 MPa and 1.46 MPa respectively.

The bubble frequency f in RPI model is given according to Cole (1960) [10] as a function of the detachment size d_W as

$$f = \sqrt{\frac{4g(\rho_L - \rho_G)}{3C_D d_W \rho_L}} \quad (2)$$

where g is gravity, ρ is density of liquid (L) and gas (G) and C_D is the drag coefficient. From Eq. 1 and 2, we can conclude that the bubble dynamics is strongly dependent on the thermal properties of the fluid and the bulk temperature. Base on the study of Tolubinsky and Kostanchuk [5], Kurul and Podowski [4] fixed the ratio between bubble growth time and waiting time to a constant of ¼.

The bubble activation, that is the activated nucleation site density (N), is expressed by a correlation given as

$$N = N_{ref} \left(\frac{T_W - T_{sat}}{\Delta T_{refN}} \right)^p . \quad (3)$$

where constants $N_{ref} = 7.94e5$ [m^{-2}], ΔT_{refN}=10 [K] and P=1.805 respectively. Again from the assessment of Krepper, it is found that N_{ref} is also case dependent. For the other parameters the previous values of ΔT_{refN} and p were found to yield satisfactory results in the overall model framework. From Eq. 3, it is clear to see the activated nucleation site density is based on wall superheat ($T_W - T_{sat}$). Accordingly, the feed heat flux Q_{tot}, applied to the heated wall can be considered as a sum of three parts:

$$Q_{tot} = Q_C + Q_Q + Q_E , \tag{4}$$

where Q_C, Q_Q and Q_E are the heat flux components due to single-phase convection, quenching, and evaporation, respectively. The details of the RPI model can be found in the literature of Kurul and Podowski [4].

II.A New Bubble Model

In this paper, we will shortly introduce a new wall boiling model [8], mainly focus on the novelty. Until today it seems that the bubble dynamics models still require some empirical constants to account for different thermal hydraulic conditions. To reduce the case dependency, a model without these constants was developed and tested. The model has a low case dependency and a high accuracy to predict the bubble dynamics, bubble departure and lift-off in pool or flow boiling. The model was built based on the on previous studies, e.g. of Colombo and Fairweather [11], Raj et al. [16] and Mozzocco et al. [17]. In 2015, Colombo and Fairweather [11] developed a mechanistic model to simulate the bubble growth and departure. In the model, they considered the contribution of the microlayer based on work of cooper and Lloyd [12], the superheated thermal liquid layer based on Plesse and Zwick [13] and the condensation evaluated from Ranz and Marshall [14] to bubble growth. Further they applied the force balanced model from Klausner et al [15] to determine the bubble departure. Based on the suggested contact angles from Klausner et al. [15] and other empirically measured contact angles, the model seems had a good agreement with data from different experiments. The bubble growth is described as an analytical solution as

$$\frac{dr_b}{dt} = \frac{1}{C_2} Pr^{-0.5} \mathrm{Ja} \left(\frac{k_l}{\rho_l C_{p,l}}\right)^{0.5} t^{-0.5} + \sqrt{\frac{3}{\pi}} k_l (T - T_{sat}) \left(\frac{k_l}{\rho_l C_{p,l}}\right)^{0.5} t^{-0.5} (1 - b) - \frac{k_l\left((2 + 0.6 Re^{0.5} \mathrm{Pr}^{0.3})(T_{sat} - T_L)\right)}{2 r_b \rho_g h_{fg}} b. \quad (5)$$

r_b is bubble radius, C_2 is microlayer constant evaluated as 1.78 by Cooper and Lloyd, k_l is liquid thermal conductivity, ρ_l is liquid density, $C_{p,l}$ is specific heat capacity, h_{fg} is latent heat, ρ_g is gas density, Ja is Jacob number, Pr is Prandt number, Re is Reynold number and b is the portion of the bubble surface in contact with the subcooled liquid.

However this model still required the empirical measured contact angle and base diameter to enhance the accuracy of prediction for different cases. In the new model which we developed [8], a dynamic contact angle method and a dynamic bubble geometry tracking method was applied to further improve the case dependency of the previous bubble model. These two models as the main novelties will be introduced in the next subsection.

II.B Novelties of the Present Bubble Model

As shown in Figure 1, after a fast expansion, the bubble's main body starts departing but as the evaporation of microlayer still produces enough vapor the main body remains connected to the wall. The base diameter of the bubble starts to shrink when the evaporation of microlayer is less than required to form a new bottleneck. Unlike in the conventional force analysis model the bubble departure or lift-off criterion is that the bottleneck breaks up or the base diameter shrinks to 0. The bottleneck breaks up is judged by the pressure difference between points A and B (Figure 1).

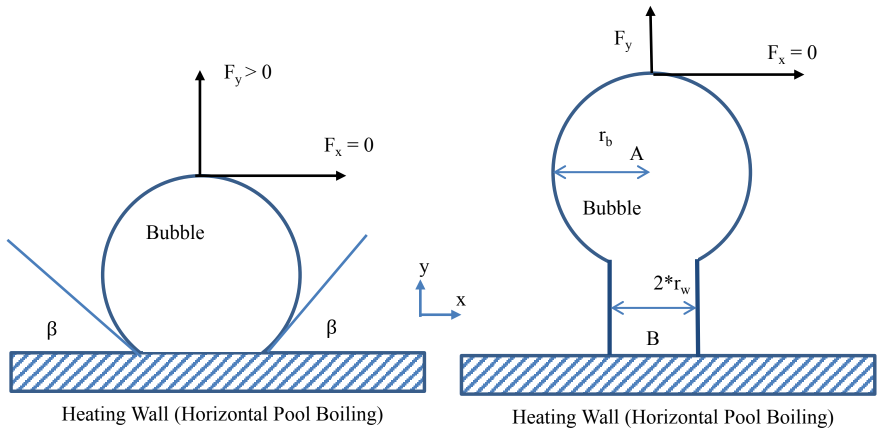

Figure 1: Formation of a bottleneck after force unbalance and before bubble departure.

$$\Delta p_{AB} = \frac{1}{2}\rho_g v_p^2 + \rho_g g h + \sigma\left(\frac{1}{r_w} + \frac{1}{r_\infty} - \frac{2}{r_b}\right). \quad (6)$$

where Δp_{AB} is the pressure difference between bubble main body and base, v_p is the bubble moving velocity of mass center, r_w is the bubble base radius, $\frac{1}{r_w} + \frac{1}{r_\infty}$ is the curvature of the contact line at the bubble base. when Δp_{AB} is larger than the total force in perpendicular direction acting on the base area, that is $\frac{|F_{total,n}|}{A_{base}}$,the bottleneck will break up and the bubble will depart from the wall. From our tests, it is found that when $r_\infty = r_w$, good agreements are got between models and experiments.

During the bubble growth, the dryout radius r_d increases when the sum of the negative forces which point towards the wall (mainly surface tension force) is much higher than the one of the positive forces preventing the bubble departure. This negative total force will drive the bubble to form a curvature and a contact angle to reduce the surface tension force in the negative direction until the forces on the bubble are balanced. The contact angle at which the force is again balanced is referred to as expected contact angle (β_s). From the force calculation this expected contact angle can be derived as

$$\beta_s = \mathrm{asin}\left(\frac{F_{growth,y} + F_{drag,y} + F_{cp,y} + F_{sl,y} + F_{b,y}}{F_{surf,y}}\right). \quad (7)$$

where $F_{growth,y}$, , $F_{drag,y}$, $F_{cp,y}$, $F_{sl,y}$, $F_{b,y}$ and F_{surf} are growth force, drag force, contact pressure force, shear lift force, buoyancy in the wall perpendicular direction and total surface tension on the bubble respectively. The contact angle β can be calculated with the base radius and the bubble radius as

$$\beta(t) = \arcsin(\frac{r_w(t)}{r_b(t)}). \quad (8)$$

It decreases from an initial value $\beta(0)=\frac{\pi}{2}$ towards the expected value β_s in some finite time interval. So the contact angle becomes dynamically during the bubble growth.

In Klausner's work, the authors considered $d_w = 2 * r_w$ as a constant of 0.09 mm. Later Thorncroft [23] adopted $d_w = 2r_b\sin(\beta)$ in order to improve the modelling accuracy. A constant ratio with bubble diameter $d_w = \frac{2r_b}{15}$ was used by Yun et al. [22]. In this work we prefer to consider the relationship between the expansion rate of base radius $\dot{r_w}$ and that of the bubble $\dot{r_b}$ instead of absolute values r_w and r_b (as in Thorncroft et al. [23]) in order to account for a smooth growth of bubble. We express the expansion rate of r_w as

$$\dot{r_w} = \dot{r_b}\sin(\frac{\pi}{2} - \beta). \quad (9)$$

The total average error of 23% between the model and different experiments shows the reliability of the present model (See Figure 2). In particular, the comparison covers different mass load, heat flux, subcooling, pressure, orientation angle, pipe design and fluid material (See Table II).

Table I: Experiments used for validation of the bubble dynamics

	Duan [24]	Klausner et al. [15]	Situ et al. [25]	Sugrue [26]	Prodanovic [27]
Fluid	Water	R113	Water	Water	Water
Orientation	Horizontal	Horizontal	Vertical	0°,30°,45°,60°,90°,180°	Vertical
Channel	Plate	Rect.; D_h = 25 mm; no full filled	Ann.; D_h = 19.1 mm sampling points at different position	Rect.: D_h = 16.7 mm	Rect.: D_h = 9.3 mm
G/kg $m^{-2}s^{-1}$	0	112-287	466-900	250-400	76.6 – 766
Q" /KW m^{-2}	28.7; 36	11-26	54-206	50,100	200 - 1000
ΔT_{sub} /°C	0.5;1	saturated	2-20	10,20	10, 20 , 30
p/bar	1.01	1.5	1.01	1.01;2.02;5.05	1.05; 2
Uncertainties from Measurement	±0.07 mm	±0.03 mm	±0.016	±0.113 mm	

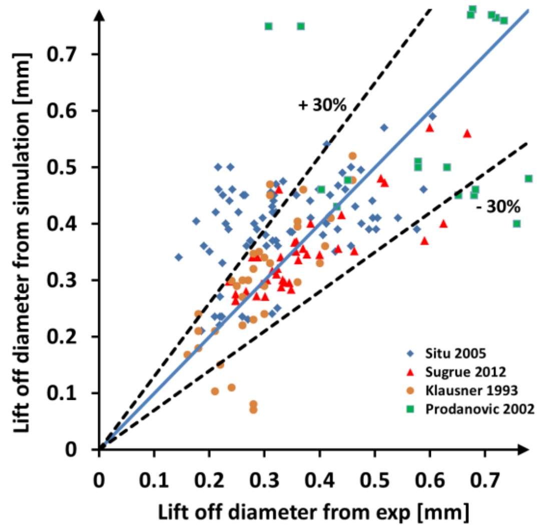

Figure 2: Comparison of the bubble lift off diameter between experiments and simulation in flow boiling under different conditions.

From the sensitivity analysis, the model can accurately reproduce the dependency of bubble departure and lift-off diameter on different impact parameters such as mass load, heat flux, subcooling temperature, pressure and orientation angle. The model confirmed the conclusions of previous works, such as that an increase of inflow velocity leads to smaller departure/lift-off diameter, higher pressure leads to smaller departure/lift-off diameter and so on. The model is even helpful to consider the contrary conclusions, e.g. that higher heat flux leads to larger departure/ lift-off diameter in Situ and Sugrue's case [25, 26] and higher heat flux leads to smaller lift-off diameter in the Prodanovic's case [27]. It was found that the increase or decrease of the lift-off diameter is strongly condition-dependent. The model is also helpful to characterize the impacts of different parameters quantitatively. Differs from the introduced RPI model, the bubble departure diameter and frequency in the new developed bubble model is a function of wall superheat.

II.C. Cavity Group Activation Model

The new single bubble model has an acceptable accuracy for both pool boiling and flow boiling under different conditions, which is preferential for CFD codes. The difference between the subcooled dependent bubble dynamics in RPI model and the wall superheat dependent one in new single bubble model troubles the implementation of the single bubble model into the EE CFD approach.

In order to consider the wall superheat dependency of the bubble dynamics in the new single bubble model, the way to implement the bubble dynamics must be updated. We simply classify the activated nucleation sites into different groups with different wall superheat. For each activated group, bubbles have the same bubble dynamics for both departure diameter and frequency with known boundary conditions, such as flow velocity and bulk temperature (See Figure 3).

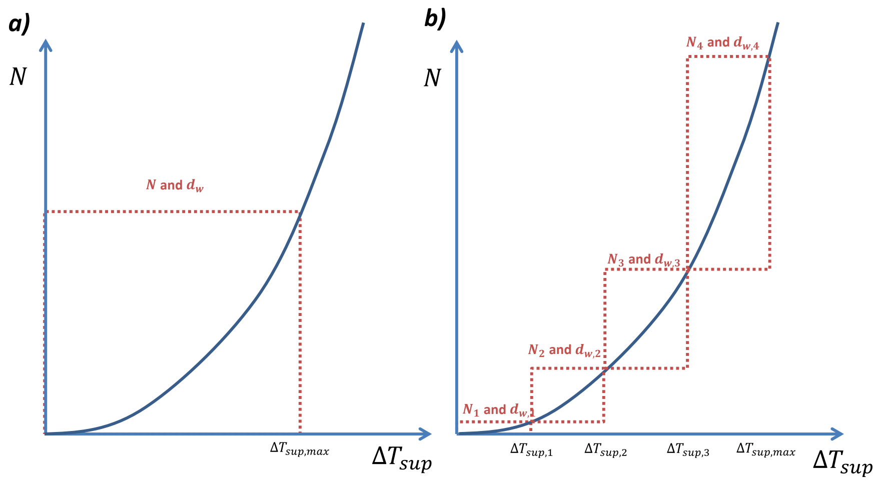

Figure 3: The Nucleation site density (N) and bubble dynamics in the conventional RPI model (a) and in the group activation model (b).

The nucleation site density N_1 is still following Eq. 3. N_2, N_3 and N_4 are calculated with Eq. 3, which can be written as

$$N_i = N_{ref}\left(\frac{\Delta T_{\sup,i}}{\Delta T_{refN}}\right)^p - N_{ref}\left(\frac{\Delta T_{\sup,i-1}}{\Delta T_{refN}}\right)^p \qquad (10)$$

where N_i is the nucleation site density at group i and $\Delta T_{\sup,i}$ is the activation superheat of group i. In this way, the bubble dynamics impacted by wall superheat will be implemented into the CFD code as the condition to calculate the heat fluxes.

II.D. Updated Heat Partitioning Model

As is introduced, the heat portioning model is employed in the conventional RPI model shown in Eq. 4. However if the group activation model is applied, the heat portioning can be simplified. If we consider the boiling as a stable process in the nucleation boiling region, it means that in the bubble influenced area (evaporative area) the time averaged heat flux due to the evaporation and quenching is always equal to the feed heat flux. In the other words, instead of the heat balance between Q_{tot} calculated by Eq. 4 and the input heat flux on the wall Q_{feed}, the heat balance between Q_{tot} and Q_c becomes dominant to the heat conservation in the CFD calculation. Due to the steady state of boiling in the bubble influenced area, it means that the average wall superheat of the evaporative area is on average constant in each activation group respectively. The wall superheat in the area of single phase convective heat transfer should be the maximum wall superheat $\Delta T_{\mathrm{sup,max}}$. This maximum value further determines the evaporative area fraction or the void fraction of the bubble on the wall and in the bulk with other conditions such as flow profile and bulk temperature.

III. VALIDATION

In order to develop reliable models for calculation of the thermohydraulic characteristics of the steam generating channels with subcooled boiling, Bartolomej et al. (1982) [28] did experimental investigations on the volumetric vapour content in vertical channels with uniform heat release over length. The experimental Cr18Ni10Ti steel channel is of 12 mm internal diameter and 2 mm wall thickness. The experiments covered different pressure, mass flux, heat flux density and inlet water temperature. The main investigated parameter was volumetric steam content which was measure by γ-radiation from a Tu-170 source. Some experiments are selected to be compared with the CFD calculations which covers mass load 405 ~ 2024 $kgm^{-2}s^{-1}$, pressure 7 ~ 15 MPa , heat flux 790 ~ 1130 KWm^{-2} and inlet liquid temperature 421 ~ 598 K (See Table III).

The simulation is carried out on the ANSYS CFX 14.5. All the model setups are referenced with respect to the Bartolomej case validation in the work of Krepper in 2007 [29]. The gas phase is considered as a mono dispersed bubble phase with bubble size between 0.05 mm to 2 mm with a subcooling dependent blending function defined in ANSYS CFX. Due to limitation of ANSYS CFX, the bubble departing from the wall into bulk is still with an averaged mono size group, which will be further improved in the new version of ANSYS CFX.

Table II Selected test cases of Bartolomej [28] under different conditions

	Pressure [MPa]	Mass flow rate [kg m^{-2} s^{-1}]	Wall heat flux [kW m^{-2}]	Inlet temp. [K]	Test no.
BART1	7	405	790	421	P7G0.405Q790
BART 2	7	965	790	493	P7G0.965Q790
BART 3	7	1467	790	519	P7G1.467Q790
BART 4	7	2024	790	520	P7G2.024Q790
BART 5	7	961	1130	466	P7G0.961Q1130
BART 6	15	1847	770	598	P15G1.847Q770

The test number was derived basing on the test parameters in the following way: P stands for pressure in 0.1 MPa, G for mass flow rate in 1000 kg $m^{-2}s^{-1}$, Q for wall heat flux in kWm^{-2} and T for the subcooling in K.

With help of the single bubble model d_{ref} is not needed to be calibrated again. However, because the nucleation site density is strongly dependent on the wall surface finishing method, which still lacks a clear description, it is still necessary to do a calibration. Here we found for the Bartlomej experiments, that N_{ref} is equal to 7.5×10^7.

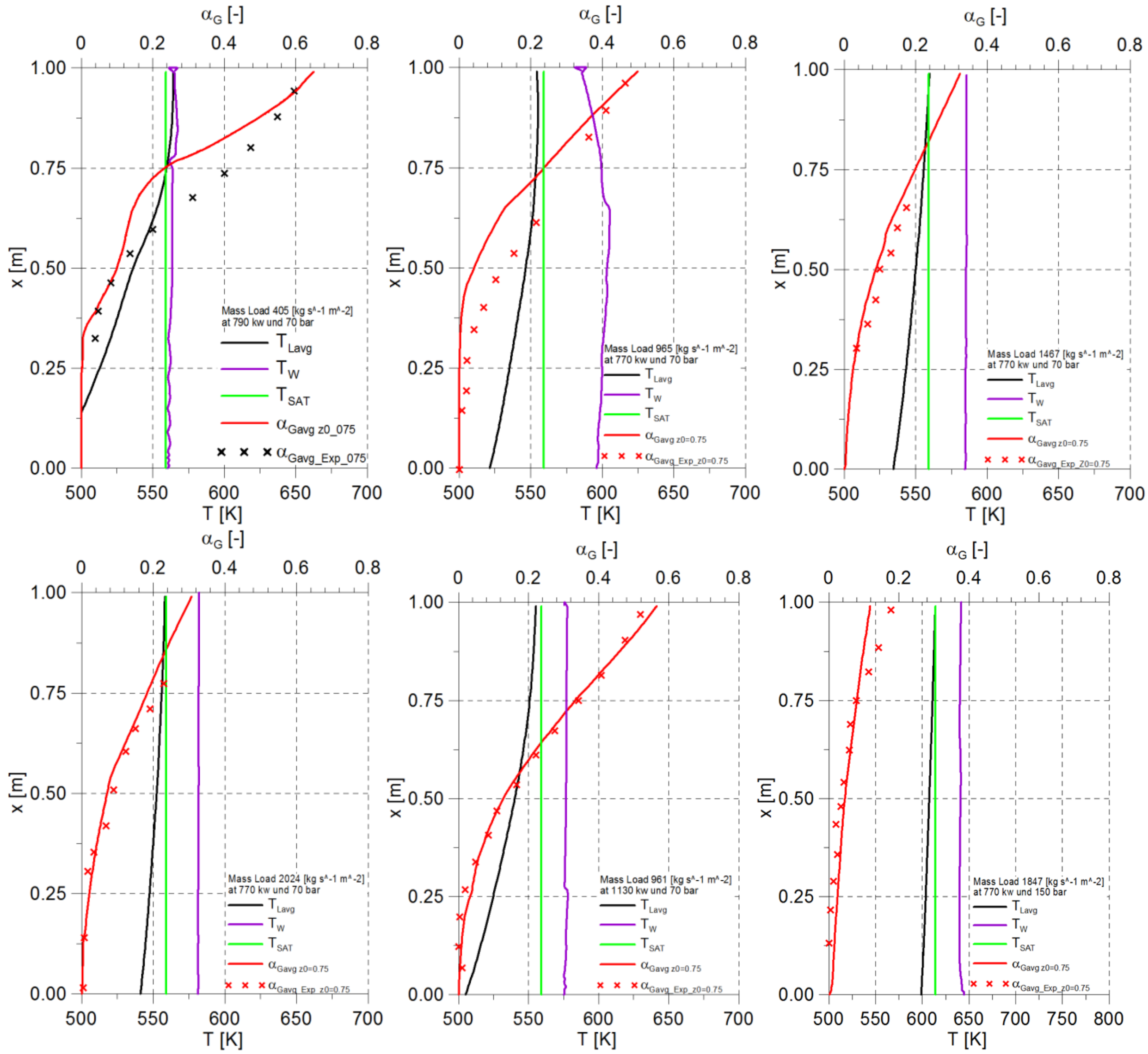

Figure 4: Comparison of simulation and experiments for cases of Bartolomej [28] given in Table II.

Of cause this good agreement between experiments and simulation in the validation (See Figure 4) is only a preliminary result for the new implemented models. More information such as the bubble population distribution in the pipe and the wall temperature is still missing. The further validation will be done with the DOBERA cases [2, 30, 31] in which the details of bubble size and wall superheat were captured.

IV. CONCLUSIONS

EE CFD approaches were widely applied in the simulation of the boiling process. However due to the employment of too many correlations, the approach becomes very specific which requires carefully recalibration such as for nucleation site density N_{ref} and departure diameter d_{ref}. In order to reduce the case dependency, a new single bubble model was developed. To implement this model requires the adaption of the approach with new activation and heat partitioning sub models. In this paper, the cavity group activation model and updated heat partitioning model were introduced. With these two models, the single bubble model can be successfully implemented in the EE CFD approach. A comparison between the experiments of Bartlomej and model shows good agreement in the void fraction with only one time calibration of nucleation site density. The good agreement shows the applicability of the single bubble model and the new developed implement submodels under different flow conditions, e.g. subcooling, feed heat flux, pressure and mass load. In the near future, with help of bubble population balanced model (inhomogeneous MUSIG [6, 32] and other submodels [2]) the approach will be extended to comparison with DOBERA cases which captured the bubble size distribution and wall superheat.

V. ACKNOWLEDGMENTS

This work is funded by the German Federal Ministry of Economic Affairs and Energy (BMWi) under grant number 1501473C on the basis of a decision by the German Bundestag.

VI. REFERENCES

1. G.H. Yeoh, J.Y. Tu, Computational techniques for multiphase flows — basics and applications. *Elsevier Science and Technology*, Butterworth-Heinemann (2012).
2. E. Krepper, R. Rzehak, C. Lifante, T. Frank, CFD for subcooled flow boiling: coupling wall boiling and population balance models, *Nucl. Eng. Des.* **255** 330–346 (2013).
3. A. Prosperetti, G. Tryggvason, Computational methods for multiphase flow, Cambridge University Press, New York (2007).
4. N. Kurul, M.Z. Podowski, Multidimensional effects in forced convection subcooled boiling, in: *Proceedings of the 9th International Heat Transfer Conference*, Jerusalem (1990).
5. V.I. Tolubinsky, D. M. Kostanchuk, Vapor bubbles growth rate and heat transfer intensity at subcooled water boiling, in: *Proceedings of the 4th International Heat Transfer Conference*, Paris (1970).

6. E. Krepper, D. Lucas, T. Frank, H.-M. Prasser, P. Zwart, The inhomogeneous MUSIG model for the simulation of polydispersed flows. *Nucl. Eng. Des.* **238**, 1690-1702 (2008).
7. E. Krepper, M. Beyer, D. Lucas, M. Schmidtke, A population balance approach considering heat and mass transfer – Experiments and CFD simulations. *Nucl. Eng. Des.* **241**, 2889-2897 (2011).
8. W. Ding, E. Krepper, U. Hampel. Evaluation of the microlayer contribution to bubble growth in horizontal pool boiling with a mechanistic model that considers dynamic contact angle and base expansion. Int. J. Heat and Fluid flow 72, pp 274-287 (2018).
9. B.A. Kader. Temperature and concentration profiles in fully turbulent boundary layers, *Int. J. Heat Mass Transfer* **24**, pp. 1541-1544 (1981)
10. R. Cole, A photographic study of pool boiling in the region of the critical heat flux. *AIChE J.* **6**. 533–542 (1960).
11. M. Colombo, M. Fairweather, Prediction of bubble departure in forced convection boiling: A mechanistic model, Int. J. Heat Mass Transfer 85 (2015) 135–146.
12. M.G. Cooper, A.J.P. Lloyd, The microlayer in nucleate pool boiling, *Int. J. Heat Mass Transfer* **12** 895–913 (1969).
13. M.S. Plesset, S.A. Zwick, The growth of vapour bubbles in superheated liquids, J. Appl. Phys. 25 (1954) 493–500.
14. W.E. Ranz, W.R. Marshall, Evaporation from drops, Chem. Eng. Prog. 48 (1952) 141–146.
15. J.F. Klausner, R. Mei, D.M. Bernhard, L.Z. Zheng, Vapor bubble departure in forced convection boiling, Int. J. Heat Mass Transfer 36 (1993) 651–662.
16. S. Raj, M. Pathak, M. K: Khan, An analytical model for predicting growth rate and departure diameter of a bubble in subcooled flow boiling, Int. J. Heat Mass Transfer 109 (2017) 470-481.
17. T. Mozzocco, W. Ambrosini, R. Kommajosyula, E. Baglietto, A reassessed model for mechanistic predition of bubble departure and lift off diameter, Int. J. Heat Mass Transfer 117 (2018), 119-124
18. B. B. Mikic, W. M. Rohsenow, P. Griffith, On bubble growth rates, Int. J. Heat Mass Transfer 13, 657–666 (1970).

19. Y. Utaka, Y. Kashiwabara, M. Ozaki, Microlayer structure in nucleate boiling of water and ethanol at atmospheric pressure, *Int. J. Heat and Mass Transfer* **57** 222 – 230 (2013).
20. D. Chen, L.M. Pan, S. Ren, Prediction of bubble detachment diameter in flow boiling based on force analysis, *Nuclear Engineering and Design* **243** 263–271 (2012).
21. N. Zuber, The dynamics of vapor bubbles in nonuniform temperature fields, Int. J. Heat Mass Transfer 2 (1961) 83–98
22. B. J. Yun, A. Splawski, S. Lo, , C. Song, Prediction of a subcooled boiling flow with advanced two-phase flow models, Nuclear Engineering and Design, 253 (2012) 351-359.
23. G.E. Thorncroft,, J.F.Klausner, R. Mei, Bubble forces and detachment models. Multiphase Science and Technology 13, (2001) 35–76.
24. X. Duan, B. Phillips, T. McKrell, and J. Buongiorno. “Synchronized high-speed Video, infrared thermometry, and particle image velocimetry data for validation of interface tracking simulations of nucleate boiling phenomena.” *Experimental Heat Transfer* **26**, no. 2 3 169-197 (2013):
25. R. Situ, T. Hibiki, M. Ishii, M. Mori, Bubble lift-off size in forced convective subcooled boiling flow, *Int. J. Heat Mass Transfer* **48** 5536–5548 (2005).
26. R.M. Sugrue, J. Buongiorno, A modified force-balance model for predicting bubble departure diameter in subcooled flow boiling, in: *Proceedings of the 15th International Topical Meeting on Nuclear Reactor Thermal-Hydraulics*, Pisa, (2013)
27. V. Prodanovic, D. Fraser, M. Salcudean, Bubble behaviour in subcooled flow boiling of water at low pressures and low flow rates, *Int. J. Multiphase Flow* **28** 1–19 (2002).
28. G.G. Bartolomej, V.M. Chanturiya. Experimental study of true void fraction when boiling subcooled water in vertical tubes, *Thermal Engineering* Vol. **14**, pp. 123-128, *translated from Teploenergetika* Vol. **14**, 2, pp. 80-83 (1967).
29. E. Krepper, B. Koncar, Y. Egorov. CFD modelling of subcooled boiling-Concept, validation and application to fuel assembly design, Nuclear Engineering and Design Vol. **237**,716-731 (2007)

30. E. Manon. Contribution à l'analyse et à la modélisation locale des écoulements boillants sous-saturés dans les conditions des Réacteurs à Eau sous Pression, PhD thesis, Ecole Centrale Paris, Nov. 2000
31. J. Garnier, E. Manon, G. Cubizolles. Local measurements on flow boiling of refrigerant 12 in a vertical tube, *Multiphase Science and Technology*, **13**, pp. 1-111 (2001).
32. T. Frank, P. Zwart, E. Krepper, H.-M. Prasser, D. Lucas, Validation of CFD models for mono- and polydisperse air–water two-phase flows in pipes, *Nuclear Engineering and Design*, **238**, 647-659 (2008).